

OBJECT S5 0716+71: FLUX - LINEAR POLARIZATION COUPLING

V. R. Amirkhanyan^{1,*}

¹*Special Astrophysical Observatory of the Russian Academy of Sciences, Nizhnij Arkhyz, 369167 Russia*

The linear polarization observations of S5 0716+71 carried out by the author in 2019–2021 were continued from December 8, 2021 to March 12, 2022. These observations confirm the author’s argument made in 2022 about a periodic dependence of the degree of linear polarization of S5 0716+71 on its optical flux. The harmonic period varies from 3 to 8 mJy in the 3 to 55 mJy interval.

1. INTRODUCTION

The object S5 0716+714 has been studied by astronomers for over 40 years. It attracted much attention due to its rapid emission variations and its linear polarization. The variations were recorded in a wide interval ranging from radio to gamma rays on time scales from ten minutes to several years. The power spectrum of the variable emission component of S5 0716+714 is close to flicker noise with no signs of a harmonic component.

Such close attention to this object is determined by several factors. Variability, undoubtedly, carries hidden information about the mechanisms of emission and the magnetic field structure of the jet. It is the jet that, when pointed towards the observer, is the main supplier of S5 0716+714 emission according to most researchers.

This blazar is a rather bright object, circumpolar at our latitudes, which allows us to carry out long series of observations. Note also that observations can be carried out with good accuracy using small instruments whose observation time is less regulated. This paper continues the work of Amirkhanyan (2022), where the author presented the optical linear polarization observation results for the well-known object S5 0716+714 and suggested that the degree of linear polarization of the object depends harmonically on its magnitude. In order to refute or confirm this claim, monitoring and investigation of this object continued.

2. OBSERVATIONS AND RESULTS

Observations of S5 0716+714 were carried out over the period from December 8, 2021 to March 12, 2022 using the same SAO RAS telescope, Zeiss-600, with the same TA3-18 equipment mounted as before. A Savart plate is used as a polaroid. In order to determine three Stokes parameters (I , Q and U) it is sufficient to carry out two exposures in two polaroid position angles with an optimal difference of 45 degrees. The polarimeter performs the set number of exposures (up to 65536) with a given exposure, changing (after each exposure) the Savart plate position angle by a preset value. The observation techniques and observational material processing methods are the same (see details in Amirkhanyan, 2022). In the period from January 17, 2019 to March 12, 2022, 4419 exposures were taken with the Zeiss-600 telescope. In the first days of observations, from January 17 to 20, the exposure time was 60 s. It was then increased to 120 s for all future observations. The observation log is presented in Table 1.

Additionally, Zeiss-1000 (Afanasiev et al., 2021) and BTA SAO RAS (Shablovinskaya and Afanasiev, 2019) S5 0716+714 observation data obtained by LSPEO SAO RAS staff were used.

The obtained light curves of S5 0716+714 and standard 5 for the entire period of observations are shown in Fig. 1. To estimate the photometric and polarimetric errors, series of standard 5 observations were used (see Fig. 1 in Amirkhanyan, 2022), which are not burdened by variability. The standard shows stable photometry (Villata et al., 1998) and zero polarization. The root-mean-square error of the standard light curve, as is the case in the first paper (Amirkhanyan, 2022), is equal to 0^m006 . The mean polarization

* amir@sao.ru

level determination error of the zero standard remains at a level of 0.0077, which turned out to be better than the computed 0.0095.

Fig. 2 shows the dependence of the linear polarization level of S50716+714 on its R -band flux. For magnitude-to-flux conversion, the calibration from the internet resource¹⁾ was used. The black squares in Fig. 2 show observations from January 17, 2019 to March 2, 2021, and the red squares show those from December 18, 2021 to March 12, 2022. The coinciding fluxes in the two series of observations are in the 10–35 mJy range. As is evident from Fig. 2, the polarization in the two series for close fluxes coincides. In the first paper (Amirkhanyan, 2022) the polarization measured in different epochs coincided in the flux region of more than 40 mJy (see Fig. 7 in Amirkhanyan, 2022). The connection of the flux with the polarization level of the object can thus be traced in a wide range of observed fluxes.

Besides the Zeiss-600 observations, the plot also shows observations of this object carried out with the following SAO RAS telescopes: BTA, February 6, 2018 (Shablovinskaya and Afanasiev, 2019) and Zeiss-1000, January 16–17, 2020. (Afanasiev et al., 2021). These observations were carried out continuously for over 8 hours with 60 s exposures. As a result, 491 and 461 flux and linear polarization measurements were obtained with the Zeiss-1000 and BTA correspondingly. These data were reduced by the author and are shown in Fig. 2 by cyan (BTA), green, and blue (Zeiss-1000). It is necessary to clarify the cross referencing procedure of the object fluxes obtained with different telescopes. While the Zeiss-600 observations were carried out in the R -band, the Zeiss-1000 observations were performed without a filter. The receiving system worked in the 4000–8500 Å wavelength interval. Early morning Zeiss-600 observations on January 16, 2020 and Zeiss-1000 partially overlap, which allowed us to match the object fluxes. The object-to-standard 5 flux ratio during the simultaneous observation interval is 1.073 times higher for Zeiss-1000 than for Zeiss-600.

The Zeiss-1000 photometry was corrected by this value. The polarization degree estimates at the same points are equal to 0.045 for Zeiss-1000 and 0.028 for Zeiss-600. The polarization difference is possibly determined by the fact that the receiving band of the Zeiss-1000 equipment is three times wider than the Zeiss-600 band. Fig. 2 shows in green the results without the polarization correction and those corrected by -0.017 in blue. The author believes that the Zeiss-600 and Zeiss-1000 data are in a rather good agreement in the 45–55 mJy flux range. The BTA observations were conducted in the g -SDSS filter. In order to place the result of these observations on Fig. 2, one must convert the flux to the R -band. This can be done if the α spectral index of the S50716+714 emission is known between the average wavelengths of the g - and R -bands ($S \sim \lambda^{-\alpha}$).

Let us determine the object flux in the g -SDSS band (mJy) as described by G. D. Wirth¹⁾:

$$S_g = 3.73 \times 10^{6.57-0.4m_g}. \quad (1)$$

Amirkhanyan (2006) obtained the dependence of the S50716+714 spectral index on flux S in filters B , V and I . Let us use the equation for filter V , which is the closest to g -SDSS:

$$\alpha = -1.6 + 0.0168S_V. \quad (2)$$

To test this dependence the author used V - and R -band photometric series from Raiteri et al. (2003) to obtain the spectral index as a function of V -band flux:

$$\alpha = -1.55 + 0.0184S_V. \quad (3)$$

Both versions give similar spectral index values, which vary in the interval from -1.3 to -1.35 depending on flux. Considering the fact that the average wavelengths of the g -SDSS and V -bands differ only slightly (5200 Å and 5500 Å correspondingly), let us change the S_V fluxes in expressions (2) and (3) for S_g obtained with the BTA and compute the R -band flux of the object:

$$S_R = S_g(\lambda_R/\lambda_g)^{-\alpha}. \quad (4)$$

Here $\lambda_g = 5200$ Å and $\lambda_R = 6400$ Å are taken from the data described on the website¹⁾. The results of these computations are shown in Fig. 2

¹⁾ See the information on the website: <https://lweb.cfa.harvard.edu/~dfabricant/huchra/ay145/mags.html>

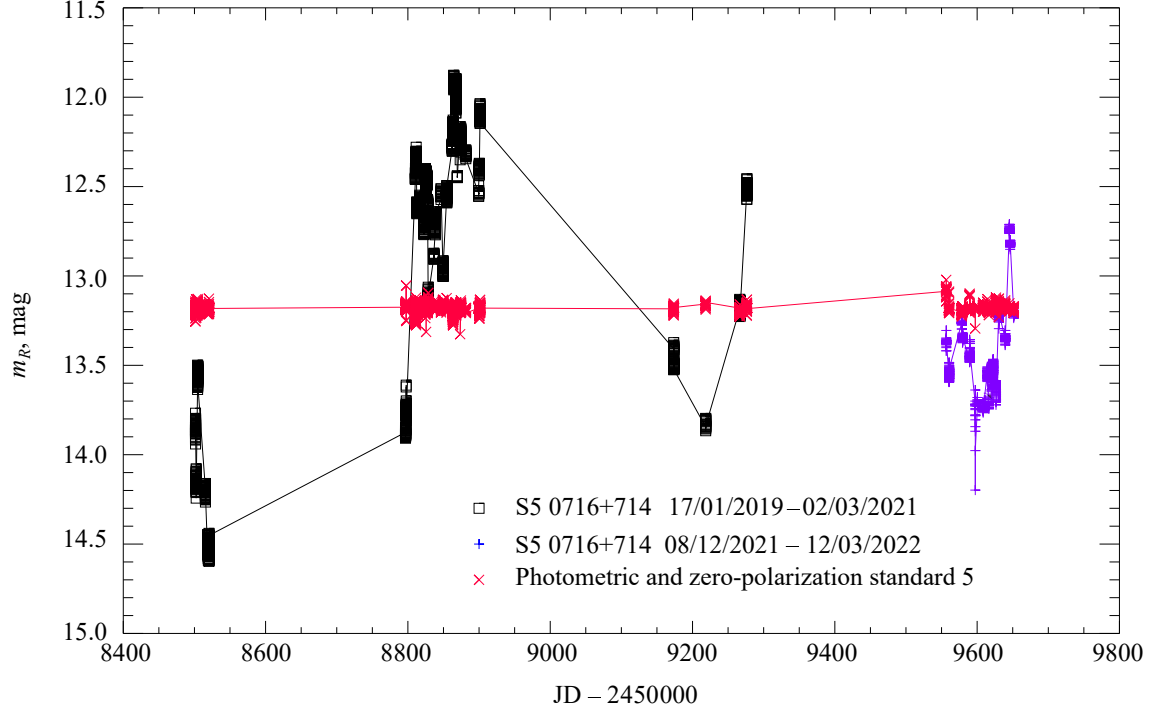


Figure 1. Light curves of S5 0716+714 and the closest standard (red line) over the entire period of observations from January 17, 2019 to March 12, 2022. The second series of observations is shown in blue.

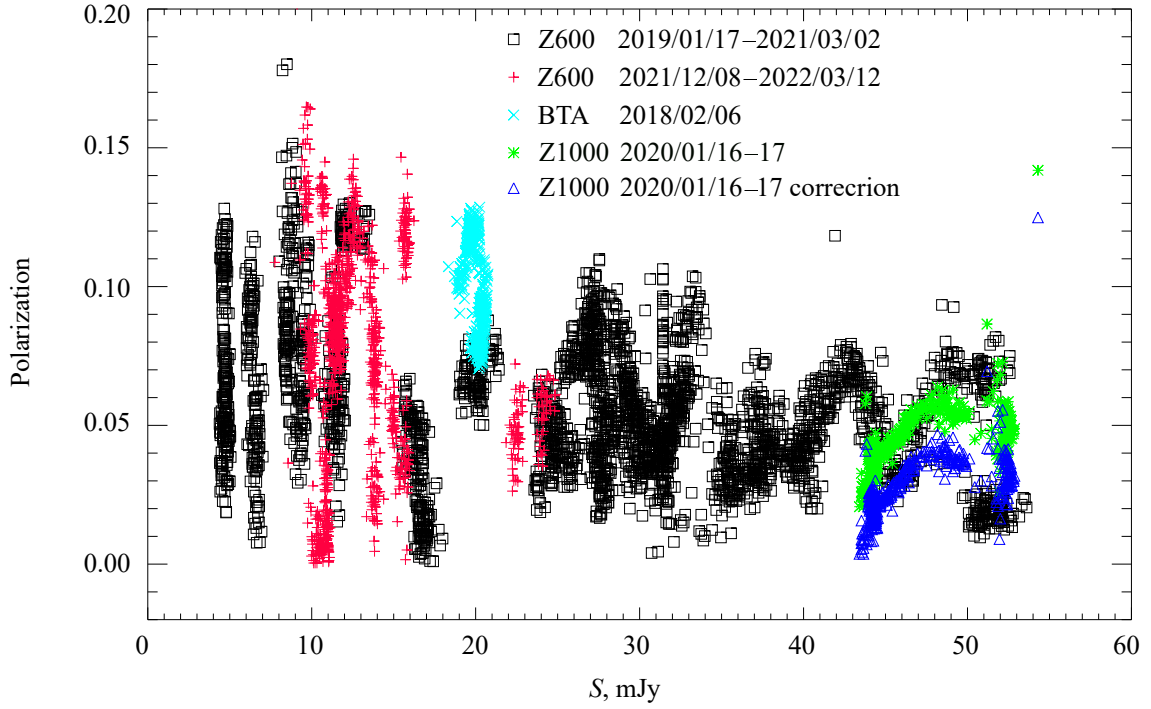


Figure 2. “Flux — polarization” dependence for S5 0716+714. Observations from January 17, 2019 to March 2, 2021 are shown in black. The red color shows observations from December 8, 2021 to March 12, 2022. BTA observations on February 6, 2018 are shown in cyan. Zeiss-1000 observations without correction carried out on January 16-17, 2020 are shown in green, and those with correction are shown in blue.

Table 1. S5 0716+714 observation log

Start of observations		End of observations		N_{exp}	Start of observations		End of observations		N_{exp}
Date	JD-2450000	Date	JD-2450000		Date	JD-2450000	Date	JD-2450000	
2019/01/17	8501.4760	2019/01/18	8501.5428	57	2020/01/20	8869.4771	2020/01/20	8869.4878	6
2019/01/18	8502.4294	2019/01/19	8502.5598	90	2020/01/24	8873.3777	2020/01/24	8873.4938	68
2019/01/20	8504.4451	2019/01/21	8504.5569	126	2020/01/25	8874.3654	2020/01/26	8874.6468	162
2019/01/31	8515.4184	2019/02/01	8515.5100	60	2020/02/01	8881.3617	2020/02/01	8881.4048	30
2019/02/03	8518.3889	2019/02/04	8518.5233	90	2020/02/19	8899.3891	2020/02/19	8899.4143	18
2019/02/04	8519.3861	2019/02/04	8519.4847	64	2020/02/20	8900.3689	2020/02/20	8900.4568	36
2019/02/05	8520.4081	2019/02/06	8520.5253	76	2020/02/21	8901.3712	2020/02/20	8901.5502	120
2019/11/09	8796.6103	2019/11/09	8796.7212	67	2020/11/20	9173.5586	2020/11/20	9173.7011	77
2019/11/10	8797.5987	2019/11/10	8797.7555	96	2021/01/04	9218.5005	2021/01/04	9218.5391	19
2019/11/23	8810.6179	2019/11/23	8810.7187	61	2021/02/20	9266.3250	2021/02/20	9266.4816	93
2019/11/24	8811.5691	2019/11/24	8811.7279	100	2021/03/02	9276.3207	2021/03/02	9276.4386	73
2019/11/25	8812.5603	2019/11/25	8812.7189	90	2021/12/08	9556.5498	2021/12/08	9556.5906	29
2019/11/26	8813.5974	2019/11/26	8813.7135	78	2021/12/12	9560.5209	2021/12/12	9560.6842	101
2019/11/29	8816.5438	2019/11/29	8816.6995	100	2021/12/29	9578.4529	2021/12/30	9578.5045	36
2019/12/05	8822.5405	2019/12/05	8822.6998	97	2021/12/30	9579.4356	2021/12/31	9579.5810	88
2019/12/07	8824.5112	2019/12/07	8824.6966	120	2022/01/10	9589.5011	2022/01/10	9589.5989	61
2019/12/08	8825.5060	2019/12/08	8825.7013	118	2022/01/17	9597.3745	2022/01/17	9597.4153	19
2019/12/08	8826.4976	2019/12/09	8826.6862	116	2022/01/20	9600.3781	2022/01/20	9600.3994	8
2019/12/09	8827.4983	2019/12/10	8827.6895	114	2022/01/28	9608.4493	2022/01/29	9608.5063	39
2019/12/11	8828.5072	2019/12/11	8828.6739	102	2022/02/03	9614.3484	2022/02/04	9614.5027	57
2019/12/18	8836.4806	2019/12/19	8836.5078	20	2022/02/05	9616.4160	2022/02/06	9616.5166	65
2019/12/20	8838.4845	2019/12/21	8838.6556	102	2022/02/10	9621.3041	2022/02/10	9621.3489	32
2019/12/29	8846.5173	2019/12/29	8846.5549	24	2022/02/11	9622.3067	2022/02/12	9622.5179	140
2019/12/31	8849.4575	2020/01/01	8849.5828	80	2022/02/15	9626.2969	2022/02/16	9626.5353	156
2020/01/05	8854.4341	2020/01/06	8854.6168	120	2022/02/19	9630.4648	2022/02/20	9630.5340	48
2020/01/13	8862.4518	2020/01/14	8862.5357	52	2022/02/28	9639.3760	2022/02/28	9639.4721	47
2020/01/14	8863.4224	2020/01/15	8863.6046	120	2022/03/06	9645.3852	2022/03/06	9645.4578	43
2020/01/15	8864.3942	2020/01/16	8864.5753	112	2022/03/07	9646.2905	2022/03/07	9646.3635	50
2020/01/18	8867.3833	2020/01/19	8867.6949	183	2022/03/12	9651.3321	2022/03/12	9651.4249	63

in cyan. The polarization values were not corrected. The author allows that the position of the cyan fragment may be shifted along the flux axis by several mJy from the real value. The upper limit of the polarization level decreases with increasing flux, which can be described by a simple expression:

$$P_{\text{max}} = 0.2(1 - 0.011S_R). \quad (5)$$

At the same time, the boundary of the polarized

part of the emission increases with increasing total flux of the object:

$$S_{P_{\text{max}}} = 0.2(1 - 0.011S_R)S_R. \quad (6)$$

In addition to the monotonic drop in the upper polarization level limit with increasing flux, a non-monotonic periodic component is evident, which repeats itself both in the Zeiss-600 observations and in the Zeiss-1000 and BTA observations.

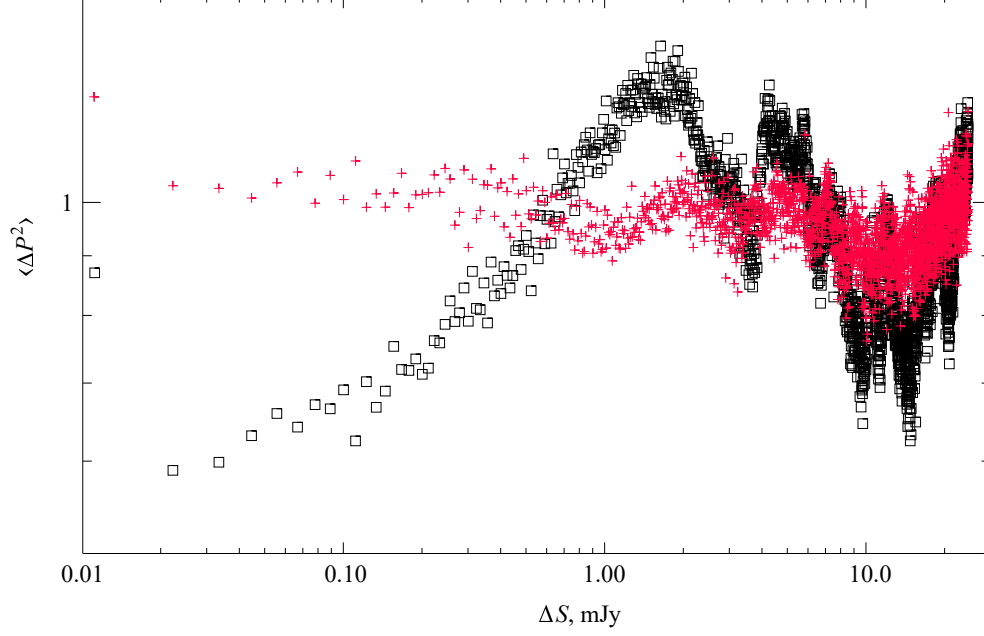


Figure 3. Black squares: structural function of the “flux—polarization” measurements obtained with Zeiss-600. Red crosses: structural function after randomizing the polarization counts.

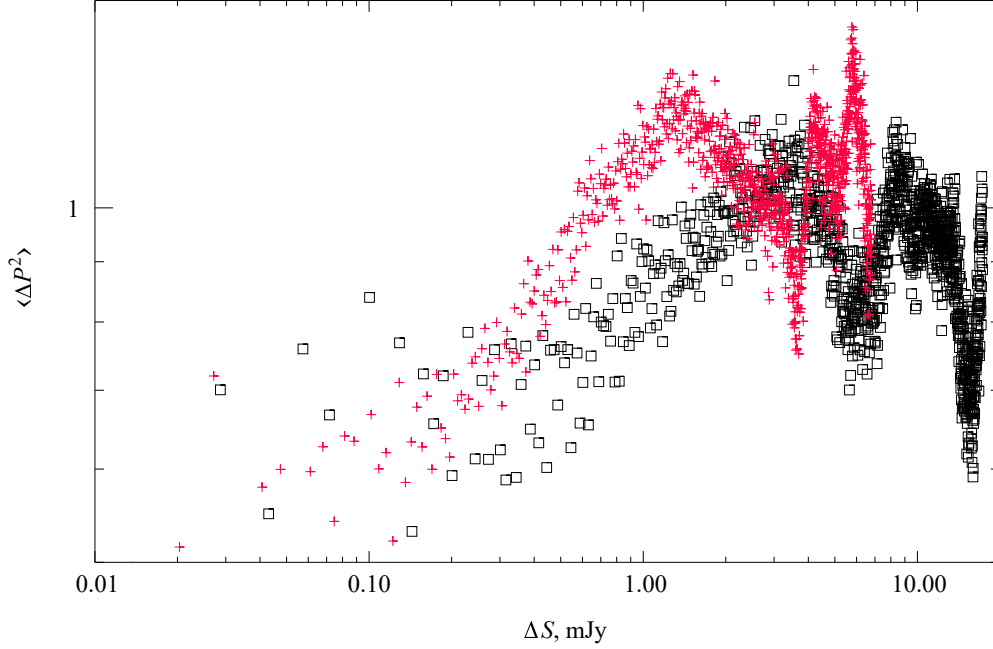


Figure 4. Structural functions for two sections of the “flux—polarization” array: the black squares show the flux above 18 mJy, the red crosses indicate flux less than 18 mJy.

To verify the last statement let us construct the following function — the root mean square variation of the polarization difference $\langle \Delta P^2 \rangle$ depending on the flux increment ΔS_R , which allows one to estimate the nature of the polarization

variations for flux counts of unequal accuracy:

$$\Delta P^2(\Delta S_R) = \langle [P(S_R + \Delta S_R) - P(S_R)]^2 \rangle. \quad (7)$$

For the structural function derivation, only the data from Zeiss-600 were used, as the most homogeneous. The graph of the structural func-

tion (Fig. 3, black squares) shows that the dependence of polarization on flux has a harmonic component. Its period is twice the position of the first maximum, the amplitude of which, ideally, tends to 2., and also twice the difference of the maximum and minimum positions of the graph.

For comparison, the result of a numeric experiment where random polarization values, distributed according to the Rayleigh law, are substituted for the real ones and shown in the same figure in red. The upper distribution boundary, as is the case in Fig. 2, is given by expression (5). If the polarization counts $P(S_R)$ are a random process, then the $P(S_R + \Delta S_R) - P(S_R)$ difference is close to stationary (Rytov et al., 1976). Therefore, $\langle \Delta P^2(\Delta S_R) \rangle$ depends only on the flux increment ΔS_R and changes little, and its error increases with increasing increment due to the decreasing number of averaged counts. Precisely this fact is demonstrated by the red plot. The same structural function for standard 5, whose polarization is determined only by the measurement errors, maintains a constant average value at the level of unity in the entire 0.01–3 mJy flux shift range, as is the case with the model function in Fig. 3. Note also an important circumstance — the number of averaged counts used in the structural function construction changes (in our case) from 2500 to 1000. Therefore, due to the central limit theorem, the distribution of the sample mean of random numbers, which is the structural function count, degenerates into a normal distribution. The theorem is true for any distribution of the initial series with a finite dispersion. The above allows one to argue that besides the monotonic component, the experimental “flux — polarization” series for S5 0716+714 also includes a variable component with a period of about 3.5 mJy.

The author divided the observations presented in Fig. 2 into two sections — from 0 to 18 mJy (2001 counts) and from 18 mJy to 55 mJy (2418 counts). For each section the structural function was constructed. In Fig. 4 they are shown by black squares (18–55 mJy) and red crosses (0–18 mJy). Evidently, a harmonic with a period of 2.5–3.5 mJy dominates in the “weak” section, and that with a period of 7–9 mJy, in

the “strong” section.

Studying multiple publications dedicated to this object allows one to find papers with the “flux — polarization degree” dependence derived, or with available observational series on flux and polarization (Ikejiri et al., 2011; Smith et al., 2009; Larionov et al., 2013; Doroshenko et al., 2017; Ahnen et al., 2018).

Our result is not confirmed in any of these papers. Although the structural function constructed using the materials of the last work shows (if one desires) the presence of a weak harmonic in the “flux — polarization” dependence. The optical observations were carried out by a wide range of telescopes, including the Crimean AZT-8 and the Saint Petersburg LX-200. At these telescopes, unlike the others, photometric and polarization measurements were made every observing night with a long series of exposures. The author does not exclude the possibility that it is these observations that left their mark on the structural function.

The author then considered the results of observations of the well-known Lacertae type type objects: BL Lac (Hagen-Thorn et al., 2002; Smith et al., 2009), 3C 279 (Kiehlmann et al., 2016), OJ287 (Villforth et al., 2010), S4 0954+65 (Morozova et al., 2014), Mkr 421 (Fraija et al., 2017). Some of these papers discuss a positive or negative correlation between the object flux and polarization degree. Rapid variations in flux and polarization are usually attributed to the superposition of the synchrotron radiation of several groups of relativistic electrons, or their motion through the entangled and regular magnetic fields. No variable component is noted in the “flux — polarization” dependence. Although the author saw an interesting picture in the graph plotted using the data from Fraija et al. (2017) (see Fig. 5). In the part where the flux exceeds 50 mJy, the nature of the graph is close to Fig. 2 and contrasts sharply with the region of weaker fluxes. This may be due to the fact that in the region of strong fluxes, observations were carried out every night from April 13 to 19, 2013 with long series of 60 second exposures, whereas only 1–2 exposures were taken per night in the region of weak fluxes.

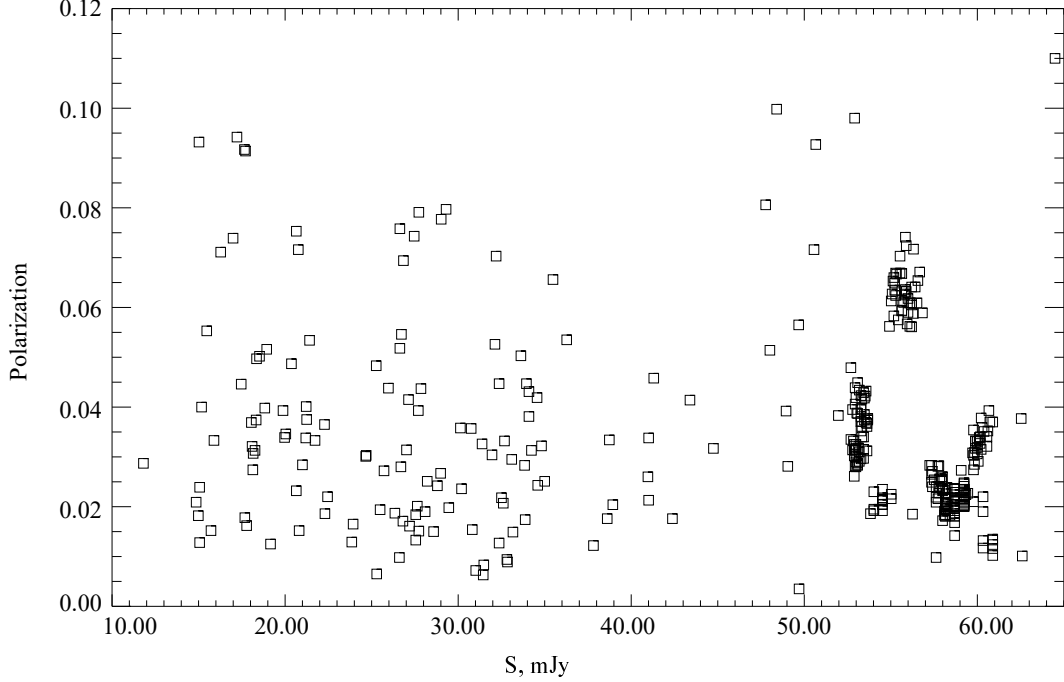


Figure 5. “Flux — polarization” dependence based on the data from Fraija et al. (2017).

3. CONCLUSIONS

Independent observations of the linear polarization of S5 0716+714 with three SAO RAS telescopes show that the “flux — polarization” relation has a harmonic component. Multi-hour series of regular exposures were performed on each night of Zeiss-600 observations. Under good weather conditions, up to 100–150 exposures were taken. Over 450 exposures per night were taken with the 6-meter (BTA) and the 1-meter (Zeiss-1000) telescopes. Detailed light and polarization curves were obtained, which allowed us to trace the variations of these parameters on scales of hours. We were able to register a harmonic connection of linear polarization with the object flux on a scale of 3–8 mJy. The absence of this effect in both S5 0716+714 and in several other objects of this type in the works of other authors seems to be due to the limited number of exposures and averaging the results of a night of observations. We shall continue observing blazars in the same regular multi-hour regime. If the effect is confirmed, then its explanation will need to be found that does not contradict the absence of a harmonic flux component, which we have been searching for in such objects for several decades.

REFERENCES

- V. L. Afanasiev, E. S. Shablovinskaya, R. I. Uklein, and E. A. Malygin, *Astrophysical Bulletin* **76** (1), 102 (2021). DOI:10.1134/S1990341321010028
- M. L. Ahnen et al. MAGIC Collab., *Astron. and Astrophys.* **619**, A45 (2018). DOI:10.1051/0004-6361/201832677
- V. R. Amirkhanyan, *Astronomy Reports* **50** (4), 273 (2006). DOI:10.1134/S1063772906040020
- V. R. Amirkhanyan, *Astrophysical Bulletin* **77** (1), 31 (2022). DOI:10.1134/S1990341322010023
- V. T. Doroshenko and N. N. Kiselev, *Astronomy Letters* **43** (6), 365 (2017). DOI:10.1134/S1063773717060032
- N. Fraija, E. Benítez, D. Hiriart, et al., *Astrophys. J. Suppl.* **232** (1), 7 (2017). DOI:10.3847/1538-4365/aa82cc
- V. A. Hagen-Thorn, E. G. Larionova, S. G. Jorstad, et al., *Astron. and Astrophys.* **385**, 55 (2002). DOI:10.1051/0004-6361:20020145
- Y. Ikejiri, M. Uemura, M. Sasada, et al., *Publ. Astron. Soc. Japan* **63**, 639 (2011). DOI:10.1093/pasj/63.3.327
- S. Kiehlmann, T. Savolainen, S. G. Jorstad, et al., *Astron. and Astrophys.* **590**, A10 (2016). DOI:10.1051/0004-6361/201527725
- V. M. Larionov, S. G. Jorstad, A. P. Marscher, et al., *Astrophys. J.* **768** (1), 40 (2013). DOI:10.1088/0004-637X/768/1/40

- D. A. Morozova, V. M. Larionov, I. S. Troitsky, et al., *Astron. J.* **148** (3), 42 (2014). DOI:10.1088/0004-6256/148/3/42
- C. M. Raiteri, M. Villata, G. Tosti, et al., *Astron. and Astrophys.* **402**, 151 (2003). DOI:10.1051/0004-6361:20030256
- C. M. Rytov, *Introduction to statistical radiophysics*, 2nd ed. (Moscow, Nauka, 1976).
- E. S. Shablovinskaya and V. L. Afanasiev, *Monthly Notices Royal Astron. Soc.* **482** (4), 4322 (2019). DOI:10.1093/mnras/sty2943
- P. S. Smith, E. Montiel, S. Rightley, et al., arXiv e-prints arXiv:0912.3621 (2009). DOI:10.48550/arXiv.0912.3621
- M. Villata, C. M. Raiteri, L. Lanteri, et al., *Astron. and Astrophys. Suppl.* **130**, 305 (1998). DOI:10.1134/S1990341322010023
- C. Villforth, K. Nilsson, J. Heidt, et al., *Monthly Notices Royal Astron. Soc.* **402** (3), 2087 (2010). DOI:10.1111/j.1365-2966.2009.16133.x